Phys. Status Solidi A **214,** No. 7, 1700275 (2017) / **DOI** 10.1002/pssa.201700275

physica status solidi a
www.pss-a.com
applications and materials science

Influence of rapid thermal processing on carrier concentration in high resistivity silicon

Luciana Capello*, Isabelle Bertrand, and Oleg Kononchuk

Soitec, Chemin des Franques, 38190 Bernin, France

Received 8 March 2017, revised 3 May 2017, accepted 3 May 2017
Published online 12 June 2017

Keywords donors, rapid thermal annealing, silicon, vacancies

*Corresponding author: e-mail luciana.capello@soitec.com, Phone: +33 476 929 537

In this study, we report changes in the carrier concentration of high resistivity Si wafers after rapid thermal annealing (RTA) anneals measured by spreading resistance technique. Spreading resistance technique (SRP) profiles clearly show the generation of donor centers with concentrations and depth distributions comparable to those of vacancy-related centers reported in the literature. Changes of carrier concentrations as a function of RTA temperature, duration, ramp down rate, and subsequent annealing in the 800–1000 °C range are consistent with the earlier literature data. The influence of annealing ambient is also studied. Annealing in pure Ar atmosphere leads to profiles dominated by in-diffusion of vacancies generated at the surface, while annealing in oxidized ambient results in well-known profiles controlled by out-diffusion of vacancies generated in the wafer bulk. Studies of the wafers with different oxygen content show that the concentration of the generated donors is directly proportional to O_i concentration.

1 Introduction It is well established that rapid thermal annealing (RTA) of silicon wafers can lead to the creation of vacancy-oxygen complexes. This phenomenon has been widely investigated in order to understand the generation of grown-in microdefects during crystal pulling [1, 2] and, more generally, the role of vacancies in various processes, such as oxygen precipitation and impurity diffusion in Si [3–5]. These vacancy-related defects have been studied indirectly by Pt diffusion or enhanced oxygen precipitation [3, 4]. Several models have been proposed to describe vacancy-related defect profiles after various thermal treatments. Thus, oxygen precipitation profiles after RTA annealing at 1250 °C with different ramp down rates can be described by a simple vacancy and self interstitial diffusion and recombination [3], while changes in such defect profiles during the subsequent anneals at 1000 °C temperature range require an introduction of vacancy agglomeration [6, 7], or most recently, the introduction of multiple vacancy species with different diffusivities [8–10]. Most of the models agree that the vacancies bind to oxygen atoms and exist predominantly in the form of VO_2 complexes at room temperature. Up to now electrical activity of vacancy-oxygen complexes resulting from RTA anneals has not been investigated experimentally. In this work, we bring new insights on vacancy-related defects by studying their electrical behavior. High-resistivity Si wafers were utilized to measure changes in the carrier concentration depth profiles after RTA by means of spreading resistance technique (SRP). The effect of different experimental conditions, such as parameters of thermal profile of RTA anneal, oxygen content, annealing ambient, Si surface state, was investigated to identify the nature of the generated defects.

2 Experimental P-type Cz 300 mm silicon wafers with resistivity ranging from 3 to 10 kOhm.cm and interstitial oxygen concentration O_i of 3 10^{17} cm^{-3} (measured by FTIR with optical calibration coefficient of 4.8 10^{17} cm^{-2}) were cleaned using standard RCA cleaning conditions prior to be subjected to RTA annealing. Surface contamination of the wafers was measured by ICP-MS technique and was found to be below 10^9 cm^{-2} for all the elements tested. RTA was performed in a lamp furnace with temperatures from 900 to 1250 °C and a soak step duration

from 10 to 90 s. The temperature ramp down rate was varied between 5 and 45 °C s^{-1}, while the temperature ramp up rate was fixed to 25 °C s^{-1}. The RTA ambient was pure Ar gas. Special precaution was taken to avoid gas contamination. The concentration of oxygen and water in the incoming Ar was below 1 ppba. Residual oxygen content in the exhaust of the RTA furnace was monitored for each run and was below the detection limit of the sensor of 1 ppma. For comparison, some samples were annealed in RTA in pure oxygen atmosphere. After RTA annealing, the resistivity profiles were measured using SRP technique and converted into free carrier concentration profiles. The conductivity type was determined at every depth point using heated SRP probe. As an example, the raw SRP data and the corresponding carrier profile are shown in Fig. 1 for wafers from the same ingot annealed at 900 and 1200 °C for 30 s in Ar ambient. The sample annealed at 900 °C was used to determine the initial bulk doping level of the ingot to avoid possible interference with oxygen-related thermodonors. Figure 1b shows the difference of the carrier concentration profiles between these two wafers. The reproducibility of SRP profiles was estimated to be at 20% from previous analysis of high resistivity samples. In this work, special care was taken in order to minimize the SRP-related errors and enable direct comparison of the results for different RTA conditions. The wafers were chosen from the adjacent positions of the ingot within few centimeters of each other, SRP tool calibration using resistivity standard and 900 °C annealed wafer was done before the measurements of each set of the wafers. The relative error in carrier concentration changes was estimated to be in the order of 5%. The SRP data points measured close to a p–n junction, if any was present, where the resistivity was above 20 kOhm.cm, were systematically omitted due to the high uncertainty in calculation of carrier concentration. The SRP samples were chosen always close to the wafer center. A slight variability of the carrier generation from ingot to ingot was observed, but the amplitude of such variation does not affect the results shown here.

In Fig. 1, we see the evolution of the Si resistivity after high temperature RTA: the resistivity has decreased and the conductivity type was converted from p-type to n-type, which can be explained only by generation of donor-like centers.

We will from now focus on the evolution of donor generation as a function of RTA conditions. In the following, the SRP data will be shown directly as generated donor concentration profiles.

3 Results

3.1 RTA of bare Si wafers Figures 2–4 show the evolution of the generated donors with RTA annealing conditions. In Fig. 2, the depth profile of the generation of free electrons as a function of the RTA temperature with a steady temperature step of 30 s is shown. The concentration of generated donors is in the range of several 10^{12} cm^{-3} and increases with the annealing temperature. In Fig. 3, the donor profile evolution with soak annealing time is reported, while Fig. 4 shows the dependence on the RTA temperature ramp-down rate. The concentration of the defects related to donor centers clearly depends on RTA soak temperature (Fig. 2): the higher the temperature, the higher the concentration which, in average, can evolve by a factor of 10. The characteristic shape of these depth profiles indicates that two components are present. In the near surface region (depth <10–12 μm) the density of the centers is reduced, most likely according to surface out-diffusion phenomena, depending on the T ramp-down rate (see Fig. 4). The bulk portion seems to follow the diffusion profile with constant surface concentration, which increases

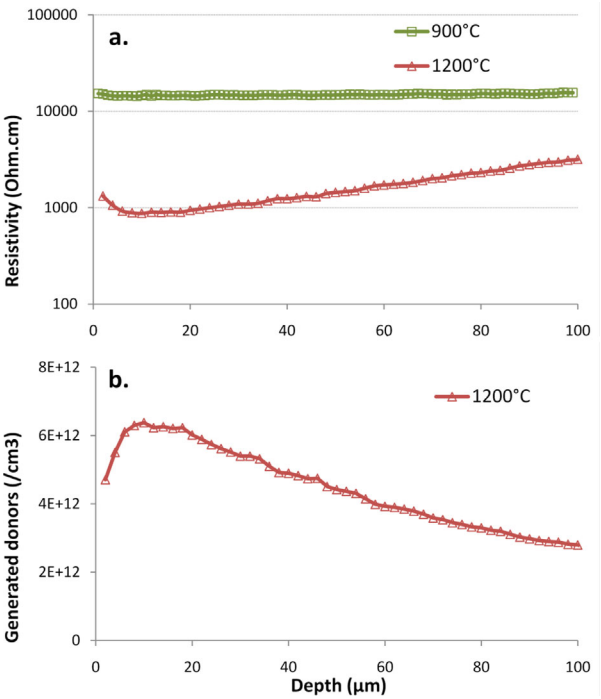

Figure 1 (a) Depth resistivity profiles on bare silicon wafers after RTA, ramp down 45 °C s^{-1}, under pure Ar, with two different temperatures: 900 and 1200 °C for 30 s. (b) Difference of carrier concentrations calculated from profiles of (a).

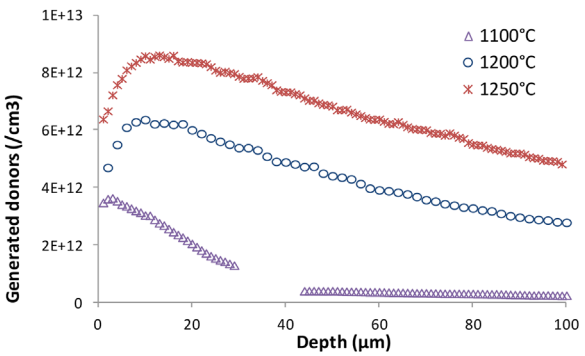

Figure 2 Depth profiles of generated donors in bare silicon wafers after RTA annealing for 30 s, ramp down 45 °C s^{-1}, under pure Ar. Missing points are intentionally omitted due to p/n junction.

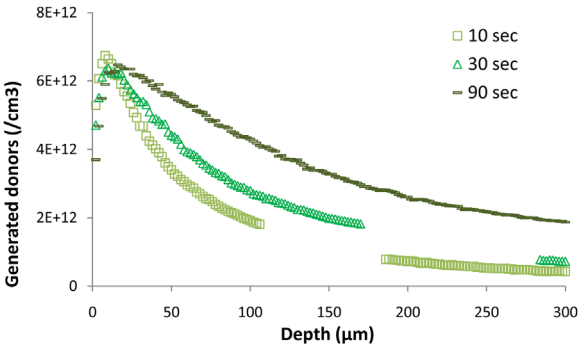

Figure 3 Depth profiles of generated donors in bare silicon wafers, after RTA at 1200 °C, under pure Ar, ramp down 45 °C s^{-1}, with different RTA durations of the steady temperature step.

with annealing temperature. From Fig. 4, one can appreciate the excellent reproducibility of the SRP measurements.

A set of experimental profiles for the wafers annealed at different temperatures for different times was simulated by solving numerically the diffusion equation with constant concentration at the surface as a boundary condition. Diffusivity and surface concentration were assumed to follow Arrhenius law with coefficients used as fitting parameters. Experimentally recorded temperature profiles were used for the simulation. As an example, Fig. 5 shows the best fit of the profiles for the samples annealed at 1200 °C. It is worth noting that we were able to fit the profiles only for the depth up to 100 μm. Deeper portions of the profiles do not follow simple out-diffusion shape. It indicates different mechanisms of donor generation in the bulk of the wafers. The best fit diffusivity and surface concentration parameters are as follows:

$$D = 1e8\ \exp\left(-\frac{4.1\ \text{eV}}{kT}\right), \frac{\text{cm}^2}{\text{s}} \quad (1)$$

$$C = 4e14\ \exp\left(-\frac{0.6\ \text{eV}}{kT}\right), \text{cm}^{-3} \quad (2)$$

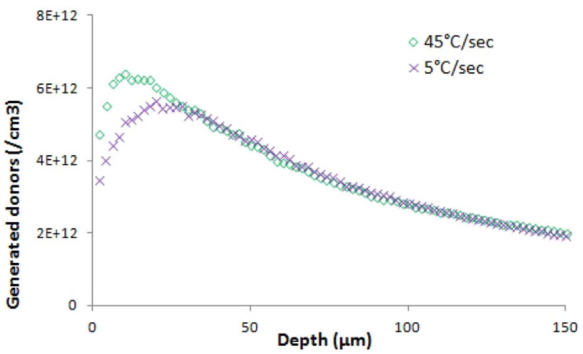

Figure 4 Depth profiles of generated donors in bare silicon wafers, after RTA at 1200 °C, under pure Ar, 30 s, with different RTA ramp down conditions.

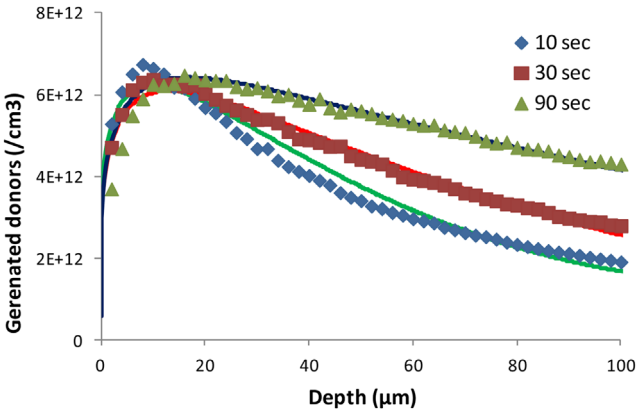

Figure 5 Depth profiles of generated donors on bare silicon wafers after RTA annealing for 30 s, ramp down 45 °C s^{-1}, under pure Ar. Solid curves are corresponding simulations.

3.2 RTA ambient and surface condition effects Figure 6 demonstrates the influence of the annealing ambient and on the donor generation for RTA annealing at 1200 °C for 30 s for different surface conditions. For annealing performed in oxygen ambient, the amount of generated charged defects drastically diminishes by about 1.5 orders of magnitude as compared to annealing in pure Ar. The level of donors generated by RTO is the lowest observed and close to the detection limit. The presence of thermal silicon oxide on the sample surface also significantly reduces the donor generation by RTA compared to native Si surface, but to the lesser extent. Moreover, the shape of the depth profile is different when we compare bare Si surface Ar anneal with RTO or RTA on oxidized surface. The concentration of the defects increases with depth for first 50 μm changing profile from in-diffusion type to out-diffusion one.

3.3 Oxidized Si wafers The behavior of oxidized silicon under Ar annealing was investigated in detail to highlight major differences to bare Si wafers. We observe an increase of the donor concentration with temperature

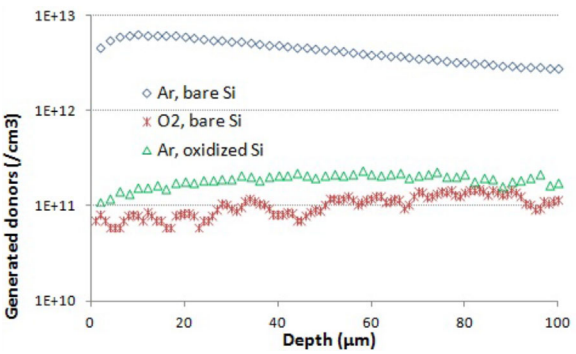

Figure 6 Depth profiles of generated donors after RTA annealing at 1200 °C for 30 s, ramp down 45 °C s^{-1}: bare surface in Ar, bare surface in O_2 and oxidized surface in pure Ar.

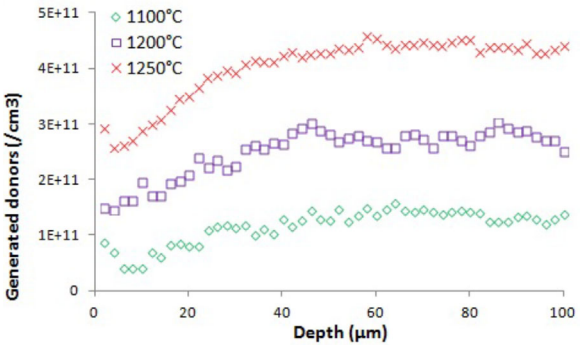

Figure 7 Depth profile of generated donors on oxidized silicon wafers, after RTA conditions under pure Ar, 30 s, ramp down 45 °C s^{-1}, with different temperatures: 1100, 1200, and 1250 °C.

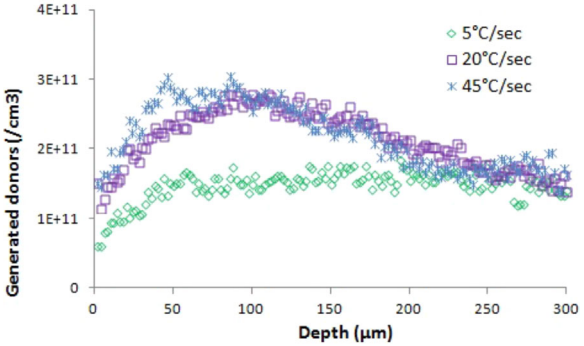

Figure 9 Donors generated in oxidized silicon wafers, after RTA in pure Ar, 1200 °C, 30 s, with different ramp down rates: 5, 20, and 45 °C s^{-1}.

(Fig. 7). The characteristic depth at which concentration reaches maximum value seems to decrease from 70 to 50 μm for 30 s RTA at 1100 and 1250 °C, respectively. In Fig. 8, the effect of annealing time is shown. The donor profile generated in oxidized samples is stable for soak time starting from 30 s and longer. Only within the first 50 μm from the surface, the concentration evolves for the first 10 s of the anneal. When looking at the effect of temperature ramp-down rate (Fig. 9), we see that the defect concentration in the bulk of the wafer (>250 μm) is independent of the ramp-rate. For high ramp rates the profiles exhibit local maximum at depth around 70 μm, while no such bump is observed for 5 °C s^{-1} cool down. The defect concentration is minimal at the surface. This behavior is very similar to the M-shaped oxygen precipitate profiles measured in Ref. [4].

3.4 Effect of interstitial oxygen Taking into account that the interaction of vacancies with interstitial oxygen is well established, we investigated an effect of RTA annealing on donor generation for sample set with O_i from 3.5 10^{17} to 1.5 10^{18} cm^{-3} (7–30 ppma "old ASTM"). One sample with O_i of 3.5 10^{17} cm^{-3} was subjected to oxygen out-diffusion anneal in pure Ar at 1200 °C for 10 h prior to RTA anneal to modify O_i profile up to the depth of 100 μm. The RTA 1200 °C for 30 s was performed in pure Ar on bare Si surface to maximize the generation of the donors. The effect of interstitial oxygen content on the generation of donor defects is evident from Fig. 10. We observe a variation in the defect density of two orders of magnitude between the depleted and the high O_i samples. The latter shows the highest charged defect density with a peak at 2.8 10^{13} cm^{-3}. The shape of the profiles is affected by the O_i content as well. The samples without oxygen out-diffusion anneal show the typical shape of the donor concentration with a near-surface out-diffusion and an in-depth diffusion profile in the bulk. In opposite, the oxygen-depleted sample has rising donor concentration with depth. Figure 11 shows donor profiles on the scales proportional to oxygen concentration. The concentration of the generated donors seems to be directly proportional to O_i concentration. The additional strong support for this assumption is shown in Fig. 12, where the ratio of donor concentrations in the samples with and without out-diffusion anneal is compared to the ratio of simulated O_i profiles using well-established O_i diffusivity values from Ref. [11]. Very good agreement between these two curves points out that the donor formation occurs at low temperatures during cool down by a formation of complexes of oxygen with defects

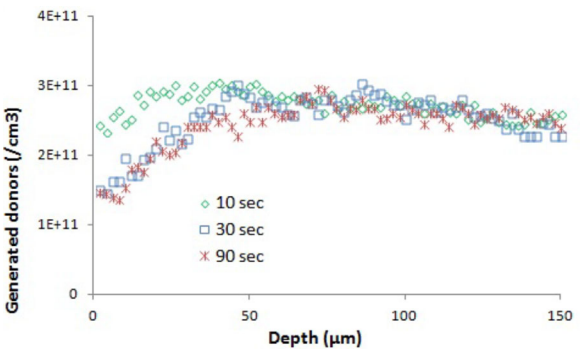

Figure 8 Depth profiles of generated donors in oxidized silicon wafers, after RTA in pure Ar, 1200 °C, ramp down 45 °C s^{-1}, with durations: 10, 30, and 90 s.

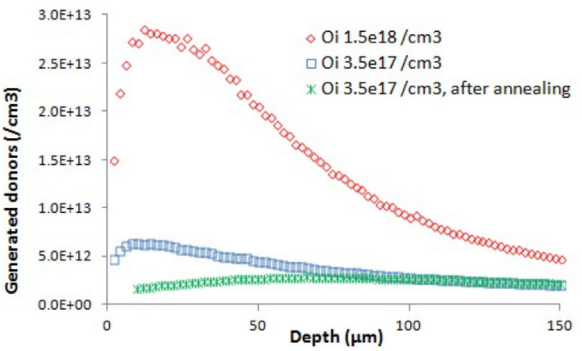

Figure 10 Depth profiles of generated donors in bare silicon wafers, after RTA in pure Ar, 1200 °C, 30 s, ramp down 45 °C s^{-1}, with different amount of O_i: 1.5 10^{18} cm^{-3}, 3.5 10^{17} cm^{-3} and wafer with O_i 3.5 10^{17} cm^{-3} subjected O_i out-diffusion annealing 10 h at 1200 °C in pure Ar.

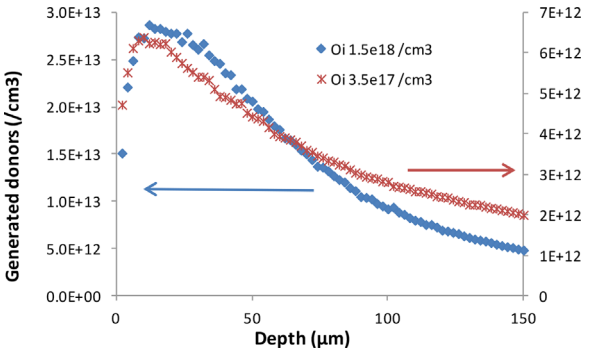

Figure 11 Data of Fig. 10 scaled proportionally to O_i concentration.

diffused from the surface during steady temperature step of RTA.

4 Discussion Based on the presented experimental data, we can argue in favor of vacancy-oxygen complexes as the origin of RTA-generated donors. First, SRP profiles clearly show generation of donor centers with concentrations and depth distributions comparable to those of vacancy-related defects reported in the literature (if we take into account difference of O_i concentration in our samples with the earlier research) [3, 4]. Their generation depends on the surface conditions during RTA. If there is injection of Si-interstitials as in the case of RTO, the phenomenon is basically suppressed. There is, however, a difference to the reported data. The donor profiles after RTA in Ar ambient resemble the vacancy-related defect profiles reported after RTA in nitrogen atmosphere, while our profiles in oxidized wafers are more close to the vacancy profiles in Ar ambient RTA. Moreover, the data of Ref. [3] suggest that during anneal in nitrogen, vacancy profiles follow a diffusion from the surface with constant flux resulting in an increase of vacancy concentration with annealing time, while our data are best described under the assumption of constant defect concentration at the surface indicating different surface conditions. The differences could be explained by different levels of Ar gas contamination. We can propose that during annealing in very pure Ar, equilibrium vacancy concentration at the Si surface exceeds its bulk value, while the addition of ppm levels of oxygen drastically reduces it. The effect of the sub ppm levels of oxygen on Si surface smoothing has been reported earlier for similar RTA anneals [12]. One can suggest that comparable oxygen levels can affect the vacancy surface concentration.

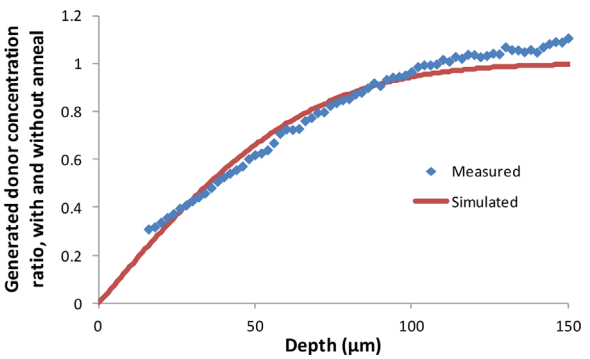

Figure 12 Ratio of generated donors for the samples with and without out-diffusion anneal. Solid curve is the simulated ratio of O_i concentrations.

Another strong argument in favor of the vacancy nature of the defects is their apparent diffusivity which is close to the literature data. The vacancy diffusivity at 1200 °C has been reported in Ref. [3] as 1.1 10^{-6} $cm^2\,s^{-1}$, which is very close to our value of 1.5 10^{-6} $cm^2\,s^{-1}$. Figure 13 shows donor diffusivity data plotted on the graph taken from Ref. [8]. A relatively high activation energy obtained in this work indicates that most probably the vacancy diffusion is affected by the vacancy-oxygen complex formation.

The fact that donor concentration is proportional to the oxygen content of the crystal is quite surprising. So far, the only reported experimental data [3] showed very little dependence of vacancy concentration on oxygen level. It should be noticed that the study in Ref. [3] addressed a very limited range of O_i (30% change only), thus, it does not allow to make unambiguous conclusions on the relation between the vacancy concentration and interstitial oxygen.

At this moment, there is not enough data to identify the exact composition of the donor centers detected in this work. We can only suggest that vacancy-oxygen complex is responsible for the donor generation.

Finally, we attempted to determine the position of the energy level associated with the donor activity. P and n-type Si wafers with resistivity in the range of 10–100 Ohmcm were annealed in RTA at 1200 °C in Ar ambient for 30 s. DLTS measurements on these samples did not show any deep levels with the concentration above 10^{11} cm^{-3}, while *C–V* data showed donor generation with concentration in the 10^{12} cm^{-3} range. This experiment points out to shallow energy position of the donor level.

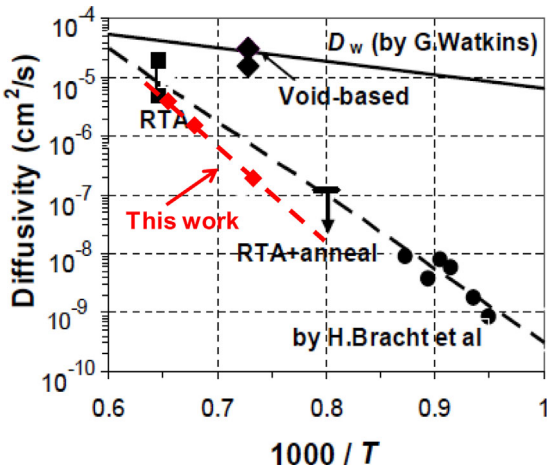

Figure 13 Apparent diffusivity of donor defects extracted from SRP data (red diamond symbols) in comparison to data from Ref. [8].

5 Conclusions We have investigated the effect of RTA annealing conditions on resistivity of Si wafers. High temperature RTA annealing leads to the generation of shallow donors. The concentration of the donors is directly proportional to oxygen concentration in Si. The apparent diffusivity of the donor centers is close to the reported in the literature diffusivity of vacancies, thus suggesting that vacancy-oxygen complex is responsible for the donor activity.

Acknowledgements The authors want to acknowledge JC Marusic and SOITEC thermal treatment process team for the support. Special thanks to Dr. T. Mtchedlidze from TU Dresden for DLTS and *C*–*V* measurements.

References

[1] V. V. Voronkov, J. Cryst. Growth **310**, 1307 (2008).
[2] T. Sinno, E. Dornberger, R. A. Brown, W. von Ammon, and F. Dupret, Mater. Sci. Eng. R. **R28**, 149 (2000).
[3] R. Falster, M. Pagani, D. Gambaro, M. Cornara, M. Olmo, G. Ferrero, P. Pichler, and M. Jacob, Solid State Phenom. **57**, 129 (1997).
[4] M. Akatsuka, M. Okui, and K. Sueoka, Nucl. Instr. Meth. B **186**, 46 (2002).
[5] V. V. Voronkov, R. Falster, and P. Pichler, Appl. Phys. Lett. **104**, 032106 (2014).
[6] T. A. Frewen and T. Sinno, Appl. Phys. Lett. **89**, 191903 (2006).
[7] J. Kubena, A. Kubena, O. Caha, and M. Meduna, J. Phys. Condens. Matter **21**, 105402 (2009).
[8] V. V. Voronkov and R. Falster, Phys. Status Solidi B **25**(11), 2179 (2014).
[9] V. V. Voronkov and R. Falster, Solid State Phenom. **205**, 157 (2014).
[10] V. V. Voronkov and R. Falster, Solid State Phenom. **242**, 135 (2016).
[11] A. Borghesi, B. Pivac, A. Sassella, and A. Stella, J. Appl. Phys. **77**, 4169 (1995).
[12] P. Acosta-Alba, O. Kononchuk, C. Gourdel, and A. Claverie, J. Appl. Phys. **115**, 134903 (2014).

